



**Pelagia Research
Library**

Pelagia Research Library

Der Chemica Sinica, 2013, 4(6):47-59



**Pelagia Research
Library**
ISSN: 0976-8505
CODEN (USA) CSHIA5

Investigations on optical and structural properties of chiral acids doped conducting polyaniline: An approach towards preeminent helicity induction

Sudha^{1*}, D. Kumar¹ and M. Iwamoto²

¹Department of Applied Chemistry and Polymer Technology, Delhi Technological University (Formerly Delhi College of Engineering), Shahbad Daultapur, Main Bawana Road, Delhi, India

²Department of Physical Electronics, Tokyo Institute of Technology, 2-12-1, O-okayama, Meguro-ku, Tokyo, Japan

ABSTRACT

Optically active polyaniline salts have been readily prepared via enantio-selective doping the emeraldine base form of polyaniline in DMF by variety of chiral dopants via suspension method. The induction of helicity is faster by dextro chiral agents than their corresponding laevo enantiomer because of the lesser energy requirement for structural deformation in dextro. CD spectra confirm the incorporation of chiral anion in PANI and helicity induction in visible region. XRD data show that PANI-(+)-HCSA and PANI-Dibenzoyl-D-Tr have orthorhombic symmetry with space group *pbcn* while the Le-Bail fit of the powder XRD pattern of PANI-(+)-Tr and PANI-(+)-Mnd confirmed triclinic symmetry with space group *P-1*. The powder X-ray diffraction patterns reveal that PANI is amorphous in nature while chiral acid doped PANI has remarkable crystallinity. SEM micrographs reveal the fibrous morphology of PANI before doping and strong coiling between the fibers of PANI after doping with chiral acids.

Key words: Chirality, conducting polymer, polyaniline, chiral dopant

INTRODUCTION

In the field of advanced materials, conducting polymers have been widely investigated to explore their unusual properties for a variety of applications [1-6]. Conjugated polymers [7-10] with external (physical, chemical, and electrical) stimuli exhibit a drastic change in their structure, shape, and morphology resulting into a newer class of materials referred as conducting helical materials. These helical materials [11-17] have been developed over the past two decades, not only to mimic biological processes but also for their attractive applications as smart or intelligent materials in analytical and biomedical fields as well as in nanotechnology [18]. However, there are only few examples of such responsive π -conjugated polymers that exhibit a change in morphology or conformation in response to chiral stimuli. In fact, chirality is a critical factor in the living systems. The living organisms consists a variety of optically active small molecules and macromolecules, which play an important role in the maintenance of life. Therefore, a pair of enantiomers, in particular chiral drugs, often shows quite different biological activities. Hence, the detection and assignment of the chirality at molecular and supramolecular levels have recently become significantly important. Thus, researchers are interested in synthesis and development of chiral conducting polymers mainly because of their tunable organic nature (by attachment of functional groups to polymer backbone) and their ability to form tailor made materials, membranes or micro- and nano-fibers. Helical polymers have many potential applications in circularly polarized electroluminescence devices, chirality modified electrodes, stereo-selective analysis for the selective transport of enantiomer [19,20], electrochemical switches, surface-modified electrodes, chiral chromatography, separation technology, sensors, chiral selectivity and molecular recognition, electrodes for

enantioselective recognition or capable of performing bio-electro-synthesis, and electrode material in organic field-effect transistors [21,22], etc.

The chirality is induced to the conjugated polymer main chain with a significant amplification resulting in the generation of either an excess right- or left-handed helical conformation, producing an induced circular dichroism (ICD) in the absorption regions of the polymer backbone [23]. In 1985 Baughman *et al.* proposed that helicity could be induced in the π - π^* absorption band of conjugated conducting polymers either by the presence of enantiomerically pure substituents or the incorporation of a chiral anion dopant onto the polymer chain [24]. Moreover, chiral anion incorporation is the best method for helicity induction as enantiomerically pure substituents are not easily available and the ease of reaction is not good. Further, chiral anion incorporation can be varied from relatively small species to large biological and synthetic polymers for successful generation of helical polymeric materials. An incorporation of chiral dopant anion is not feasible for all conjugated systems such as polypyrrole, polythiophene because of the presence of S- and N- site within the polymer ring causes an electronic and steric hindrances. It is quite possible in polyaniline (PANI) because chiral dopant anion attacks at N- (the imine and amine sites) present in the polymer chain. Hence, chiral polyaniline and its derivatives have been synthesized usually either by co-dissolving PANI or a chiral acid (HA) in a common solvent [25]. The optical activity may arise from the formation of PANI-(+)-HA product in which the chiral dopant anion induces a predominantly one-handed helical packing of essentially planar PANI chains into a chiral superstructure as reported earlier [26-30]. The chiral dopants selected to generate optically active PANI salts should be bidental in nature because it facilitates the attachment of dopant to the polymer backbone at two sites, i.e., amine and imine simultaneously.

On perusal of the literature we found that the researchers have been working on the generation of helicity in PANI chains but none of them explained the kinetics of helicity and the structural/conformational changes after induction of helicity till to date. Keeping this view in mind, we mainly focus on the factors (type of dopants, enantiomeric effect, crystallinity, visual changes with respect to experimental results) associated with induction of helicity in the PANI chain and the reason behind the difference in optical activity induction and doping level obtained by the use of dextro and laevo agents. This paper also presents the factors associated with the random use of enantiomeric HCSA among chiral agents being used worldwide.

MATERIALS AND METHODS

Chiral dopants such as D(-)-Tartaric acid, L(+)-Tartaric acid, Dibenzoyl-D-tartaric acid anhydrous, R(-)-Camphorsulphonic acid and S(+)-Camphorsulphonic acid (HCSA) were purchased from Himedia Laboratories Pvt. Ltd while S(+)-Mandelic acid and R(-)-Mandelic acid were procured from Sigma Aldrich Chemicals Pvt. Ltd. Bangalore, India. Aniline and HCl were supplied by CDH Chemicals India, while ammonium persulphate (APS) was purchased from Merck India. Dimethylformamide (DMF) was procured from Qualigen India. Aniline monomer was distilled under reduced pressure and stored at low temperature prior to its use. Other chemicals were used as received without further purification. Double distilled and demineralized water from Millipore was used throughout the studies.

Synthesis of Polyaniline

Aniline was polymerized to PANI by chemical polymerization method with the aid of ultrasonic waves using ultrasonicator at 37 ± 3 kHz frequency. A solution of freshly distilled aniline (0.2M) was prepared in 1M HCl solution. This solution was cooled at $0-5^\circ\text{C}$ and an equimolar aqueous solution of APS (0.2M) was added drop wise (2.5 μl in one lot) under sonication for 30 min keeping the temperature below 5°C . A dark green precipitate so obtained was filtrated and then washed by 1M HCl solution several times followed by deionised water. It was finally dried, and powdered. The final product was dedoped by 1:1 aqueous ammonia solution for getting emeraldine base (EB) form of PANI.

Doping of Emeraldine Base

Doping of PANI emeraldine base with all chiral acids to generate the optically active PANI salts was carried out in-situ with the aid of ultrasonic waves. PANI emeraldine base (1mg) was added to 10 ml of DMF solvent and then subjected to sonication at 37 ± 3 kHz frequency for 15 min. Then, different chiral dopants like D(-)-Tartaric acid, L(+)-Tartaric acid, and Dibenzoyl-D-tartaric acid anhydrous with concentration 0.5 mol/dm^3 and R(-) camphorsulphonic acid, S(+)-camphorsulphonic acid, S(+)-Mandelic acid and R(-)-Mandelic acid with concentration 0.05 mol/dm^3 were added into the emeraldine base solution separately and kept each sample for 30 min below 5°C under ultrasonic waves. After filtering these solutions through a $5.5\times 10^{-8} \mu\text{m}$ filter, the UV-Visible and Circular Dichroism spectra of deep green solution of polyaniline salts were immediately recorded. Finally, the filtered solutions were kept at room temperature for complete precipitation for further studies.

Characterization

UV-Visible spectra of doped solutions were recorded using a double beam UV-Vis spectrophotometer (Model UV5704SS) ECIL, India over the range of 250-900 nm. FTIR spectra of all the samples were recorded in transmission mode with KBr pressed pellets using a Perkin-Elmer (Model No.2000, UK) spectrometer. Circular Dichroism spectra of the solutions were recorded at chira-scan circular dichromator. XRD scans for PANI emeraldine base and chiral acids doped PANI were recorded using a Rigaku miniflex diffractometer employing $\text{CuK}_{\alpha 1}$ radiation at a scan rate of $1^\circ/\text{min}$ and step size 0.02 from 2θ range $5-60^\circ$. Scanning electron micrographs were obtained with a Hitachi scanning electron microscope (Model S-3700N) at an acceleration voltage of 10 kV. All samples were plasma coated with a thin layer of gold to provide electrical conduction and to reduce the surface charging.

RESULTS AND DISCUSSION

The doping of emeraldine base form of PANI with different chiral agents induces the helicity in the PANI. Fig. 1 shows the structures of all the chiral acids being used in the present study. Fig. 2 presents a scheme for the interaction of emeraldine base form of polyaniline with a chiral acid in organic solvent, viz, DMF. Since, the chiral dopants selected to generate optically active PANI salts are enantiomeric and bidental in nature, they facilitate the attachment of dopant to the polymer backbone. The chiral dopant anion used in this scheme is (+)-HCSA. A similar interaction is also believed with other chiral dopants. The optically active PANI samples have been characterized by UV-Visible, FTIR, CD, SEM and XRD techniques for detailed investigations.

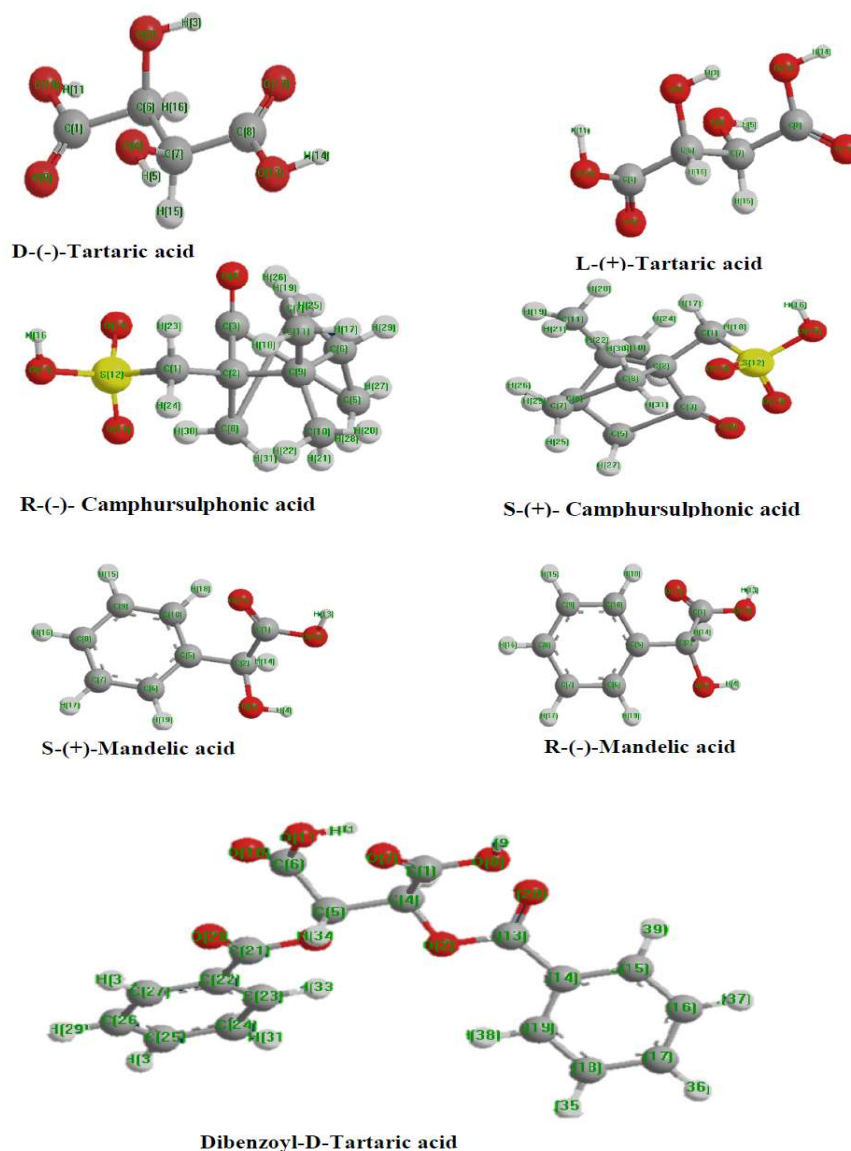


Fig. 1. Chemical structure of different chiral acids used for doping of PANI

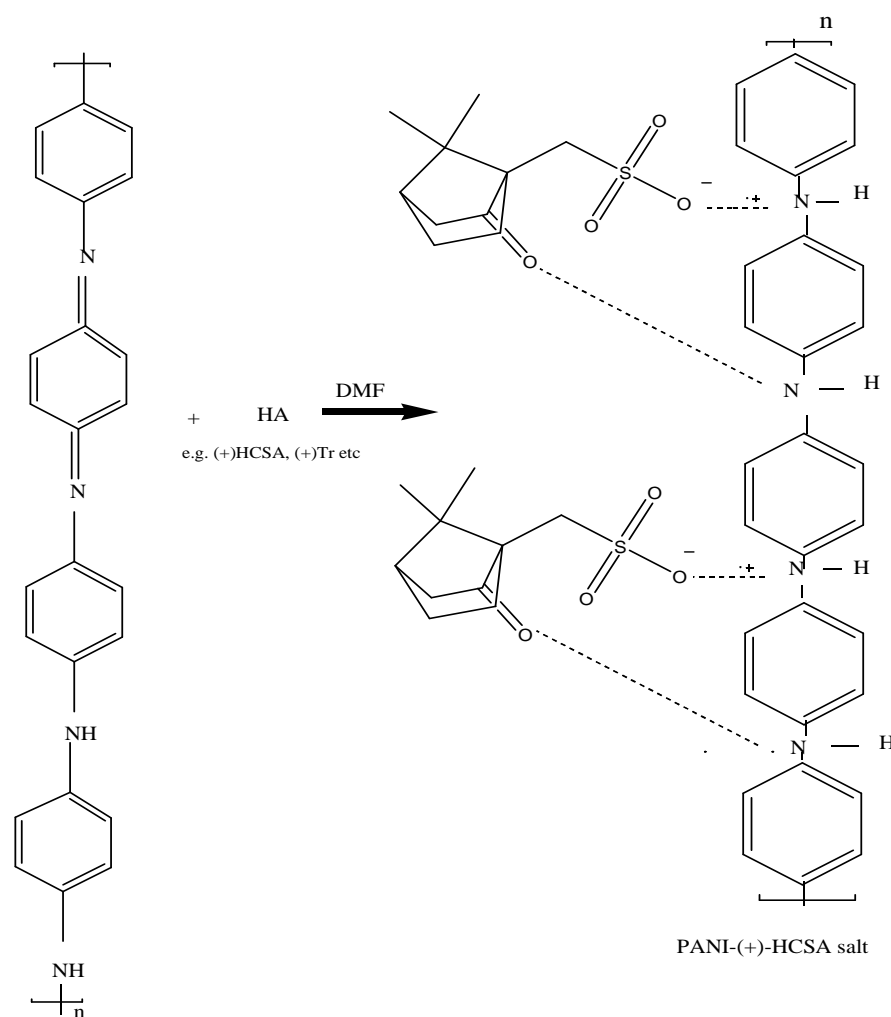


Fig. 2. Scheme for Doping of PANI emeraldine base with (+)-HCSA in DMF

UV-Visible spectroscopy

UV-Visible spectra (Fig. 3) of emeraldine base form of PANI in DMF show the characteristic excitation band at 617 nm and a π - π^* band at 355 nm. With the addition of chiral dopants to the solution, a color change from blue to green exhibits structural/conformational changes in PANI samples which is evident from the shift in absorption bands recorded in the spectra. In case of PANI(+)-HCSA, absorption bands have been observed at 344, 417 and 861 nm showing a π - π^* band and two polaron bands with “compact coil” conformation. Similarly, other chiral acids doped PANI also show the transitions corresponding to compact coil conformation and these data values have been presented in Table-1. The characteristic band shift in UV-Visible spectra shows the level of doping. It is observed that the dextro enantiomer dopant is more efficient than laevo enantiomer dopant hence the bands obtained in UV-Visible spectra are different which is clearly seen by observing a red shift. The position and intensity of the UV-Visible absorption bands of chiral acid doped PANI is related to the conformation and conjugation length of polymer. The localized polaron band in the range of 750-850 nm is considered as the characteristics of the “compact coil” conformation for the PANI chains which is found in agreement with the literature reported earlier [31].

The band gap, i.e., the difference between conduction band and valence band energy of the different chiral acid doped PANI has been calculated by using the Tauc's relationship [32]

$$\alpha = \frac{[k(h\nu - E_g)^{n/2}]}{h\nu}$$

Where, α is the absorption coefficient and E_g is the energy band, $n = 1$ (for PANI and its derivatives) is a constant and $h\nu$ is the incident photon energy. The band gap (E_g) is obtained plotting $(\alpha h\nu)^2$ vs $(h\nu)$ and extrapolating a tangent on the X-axis.

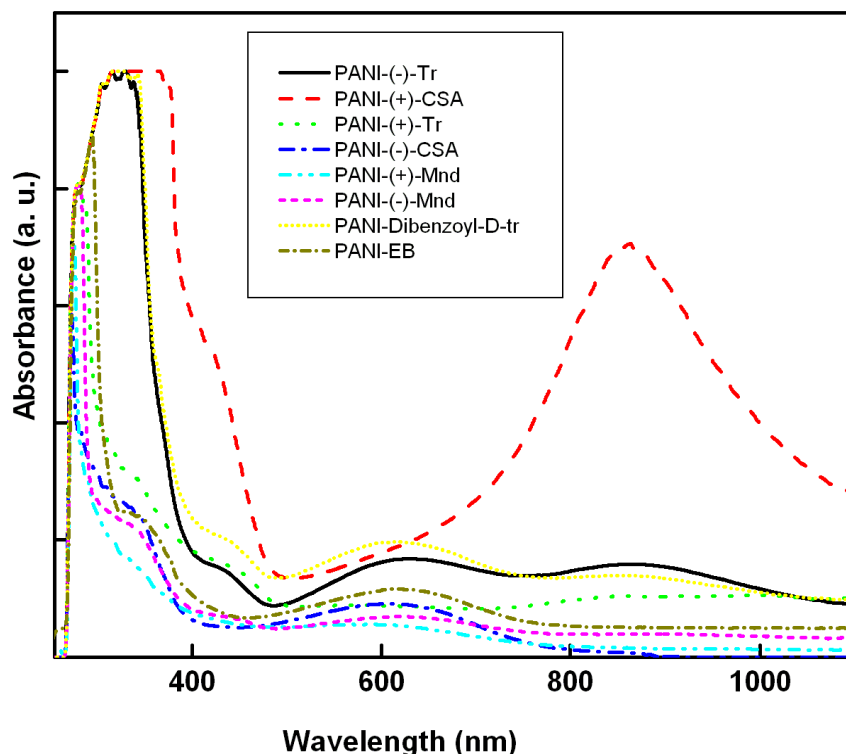


Fig. 3. UV-Visible spectra of chiral acid doped PANI in DMF

Table 1. λ_{\max} for UV-Visible and CD spectra with band gap of chiral acid doped PANI

S. No	Chiral Dopant	Wavelength λ_{\max} (nm) (UV)	Band Gap (eV)	Wavelength λ_{\max} (nm) (CD)
1	L(+)-Tartaric acid	328, 432, 632, 864	0.84, 2.39	260,387,457,777
2	D(-)-Tartaric acid	280, 440, 608, 915	1.47, 2.52	260,381,760
3	S(+)-Mandelic acid	275, 382, 579	0.93, 2.46	264,330,521,672
4	R(-)-Mandelic acid	336, 438, 630	1.62, 2.86	252,275,390,446,508
5	S(+)-Camphorsulphonic acid	347, 424, 859	0.91, 2.42	295,448,750,798
6	R(-)-Camphorsulphonic acid	270, 339, 614	1.66, 2.83	295,445,752,798
7	Dibenzoyl-D-tartaric acid anhydrous	321, 440, 611, 870	1.79, 2.41	265,335,397,446,601,741
8	PANI (EB)	296, 355, 617	1.59,3.05, 5.03	N/A

It is noticed that the band gap of right handed enantiomer is lower than its corresponding left handed enantiomer. The induction of helicity and change in color from blue to green in PANI by dextro chiral agent is faster as compared to laevo chiral agent. It resulted with time that dextro dopants change the color faster than laevo agent as color change in polyaniline is also an indicator of change in doping level. It may be predicted that the orientation of amine and imine in the polymer is almost in the similar plane as of dextro agent's polar sites. Thus, the attack of dextro agents is easy, faster and more efficient while the probability of attack of laevo is less and hence the degree of incorporation of laevo agent at the attacking site in polymer is poor. So, the concentration of laevo agents attacked at the polymer backbone and doping level is also less. The visual observation is clearly demonstrating that the band gap of dextro enantiomer is lower than their corresponding laevo enantiomer. It seems that some forces like Van der Waal's forces/hydrogen bonding do exist during induction of helicity due to which dextro conformation binding on PANI chain requires little effort and being in the same plane of attack, it needs less energy. Here, dextro conformation has lesser band gap so the structural deformation is faster and it can easily bind on the PANI chain. So, there is an extension of conjugated path leading to the lesser band gap as compared to the laevo enantiomer [33]. It is clearly seen from the Table 1 that there is a continuous decrease in band gap of PANI after doping with chiral acids. Therefore, we can conclude that the chiral acid doped PANI salt is more conducting in comparison to the PANI emeraldine base.

FT-IR Spectra

Fig. 4 shows the FT-IR spectra of PANI and doped PANI using chiral acids. The characteristic peaks are observed at 3392, 2922 and 1302 cm^{-1} which attribute due to the $-\text{NH}$ stretching, C-H stretching on aromatic ring and C-N stretching while peaks at 1498 and 1590 cm^{-1} show the presence of benzenoid and quinoid structures, respectively.

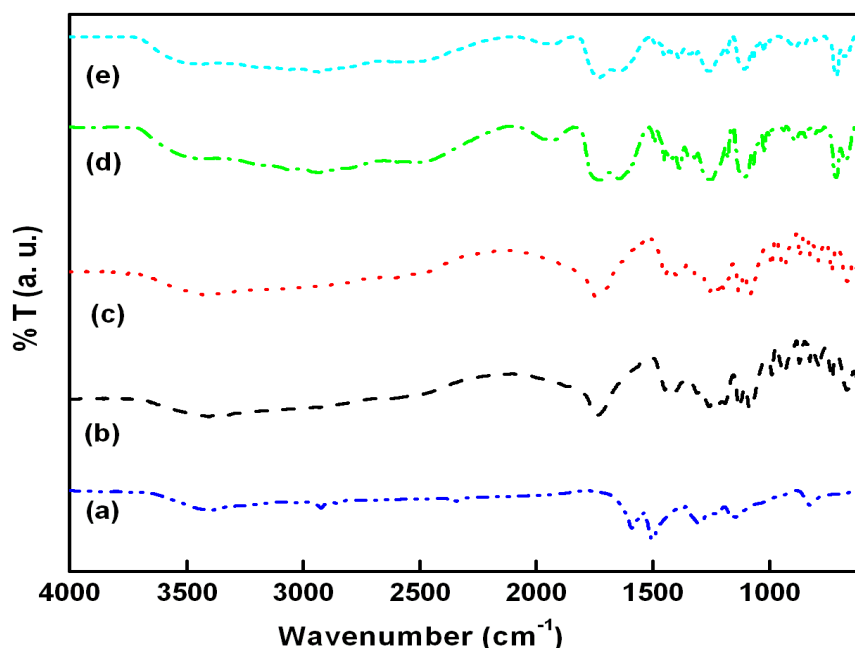


Fig. 4. FTIR spectra of (a) PANI-EB (b) PANI-(+)-Mnd (c) PANI-(+)-Tr (d) PANI-(+)-CSA (e) PANI-Dibenzoyl-D-Tr

The characteristic peak at 1165 cm^{-1} is due to an aromatic amine stretching. The peak at 828 cm^{-1} attributes due to the out of plane hydrogen deformation of aromatic rings in PANI unit sequences. The characteristic peaks of (+)-HCSA appear at 1397 and 669 cm^{-1} which are found to be in close agreement with the data reported in literature [34]. It is observed that the FT-IR spectra for PANI-(+)Tr and PANI-(+)Mnd are found to be similar.

Circular Dichroism (CD) Spectra

The most sensitive method for studying the chiroptical behavior of chiral molecules is circular dichroism spectroscopy, which measures the difference in molar extinction coefficients when passing left and right handed circularly polarized light through a sample of the compound ($\Delta\epsilon = \epsilon_L - \epsilon_R$). Most of the time enantiomeric molecules exhibit mirror image CD spectra of opposite sign. The generation of optical activity is due to an enantioselective interaction of emeraldine base with chiral acids. Most significantly distinctive CD bands observed for different chiral acid doped PANI salts are tabulated in Table 1. The CD bands are found to be correlated with UV-Visible absorption bands. The mirror imaged CD spectrum of chiral doped PANI indicates that protonation/doping of EB is enantioselective, with one or other helical screw of polymer chain being adopted, depending on which hand of the chiral anion is incorporated. It is also reported in the literature that the CD signals are observed in the range of 200-300 nm because of the attack of dopants and their activity on the PANI main chain. These dopants do not show any band in visible region, hence the bands obtained in visible region are due to the compactness and coiling of polymer backbone [35]. The intensity of dopant incorporation and coiling is much different due to an induction. Since induction of helicity is dependent upon number of chiral ions attacking at amine or imine site of PANI. As the plane of dextro ion is fit for attack at amine and imine site of PANI than laevo, the degree of rotation and % of doping is more in case of dextro. In situ generated PANI-(+)-HCSA solutions give characteristic bands at ca. 295 and 445 nm. The band at 295 nm is attributed due to the (+)-HCSA incorporated in the polymer, whereas the 448 nm band is attributed due to the optical activity induced in the polymer backbone.

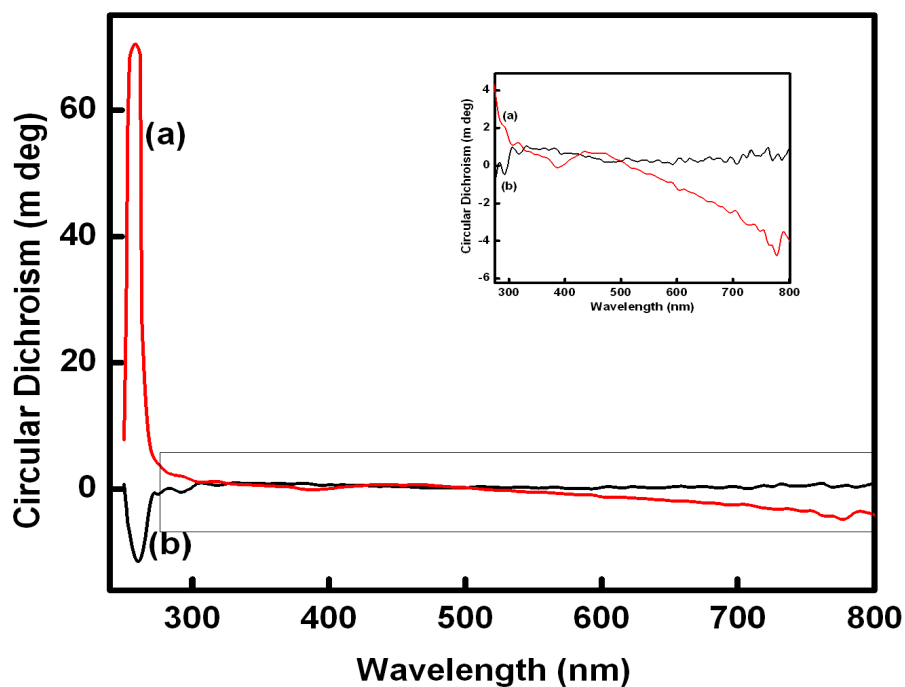


Fig. 5. CD spectra of (a) (+)-Tr and (b) (-)-Tr acid doped PANI in DMF

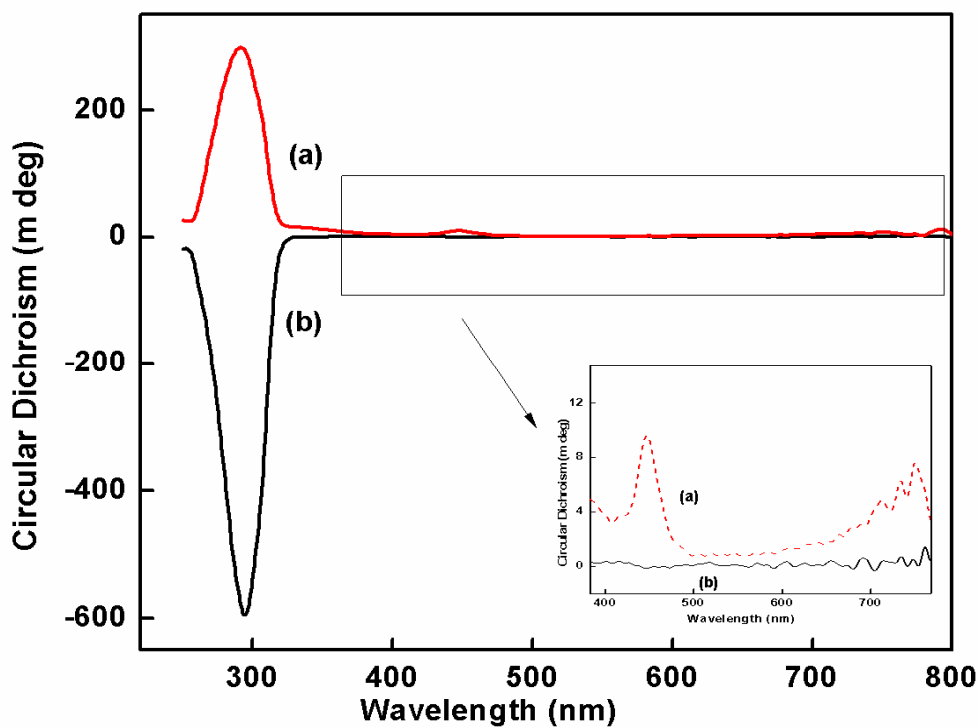


Fig. 6. CD spectra of (a) (+)-HCSA and (b) (-)-HCSA acid doped PANI in DMF

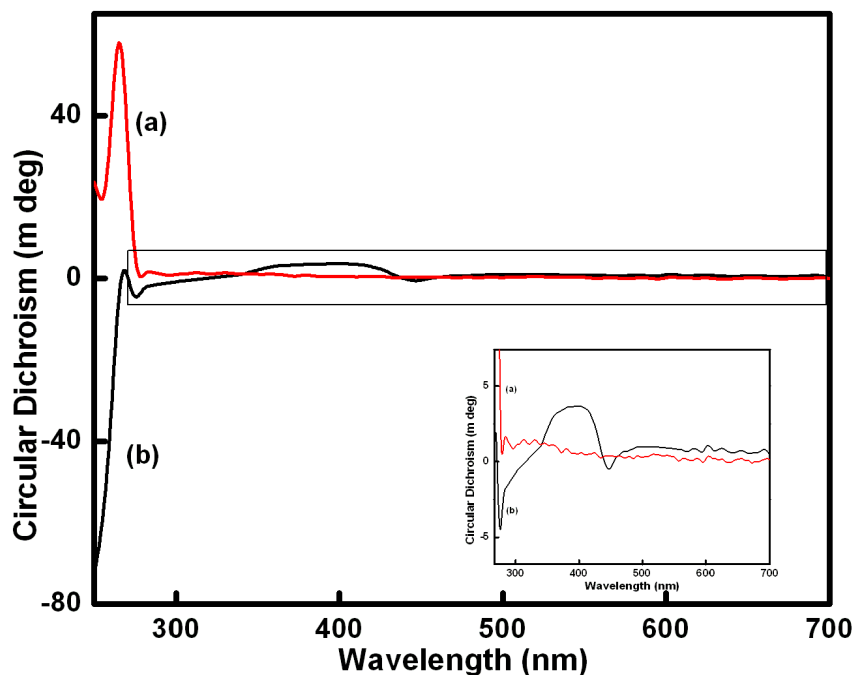


Fig. 7. CD spectra of (a) (+)-Mnd and (b) (-)-Mnd acid doped PANI in DMF

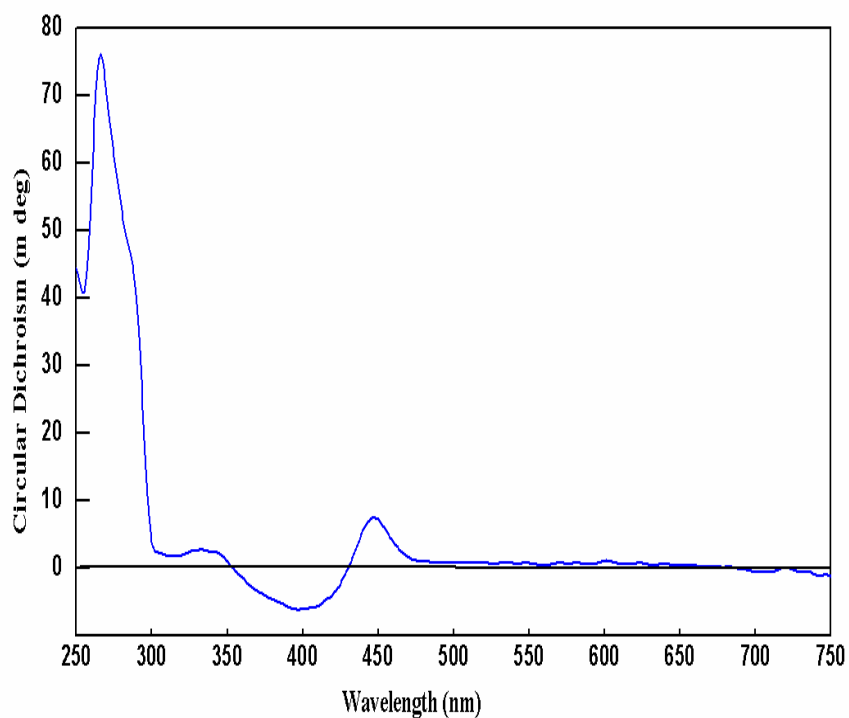


Fig. 8. CD spectra of (a) (+)-O'O-Dibenzoyl-Tr acid doped PANI in DMF

Fig. 5 to Fig. 8 shows that the extent of helicity is dependent on the number of chiral anions incorporation. The chirality of main chain is also visible from the bands obtained between 300 to 700 nm as there is symmetric difference in the induction. All these results were reported under inert atmosphere and therefore a change in degree of rotation is only because of the incorporation of dopant ions and induction of helicity in the polymer backbone. The incorporation of CSA anion is faster and better than other anions so most commonly used acid to date is (1*S*)-(+)- or (1*R*)-(-)-10-camphorsulfonic acid (HCSA), leading to the optically active solutions of PANI-HCSA salts from which chiral polymer films can be readily cast.

Powder X-ray Diffraction

The powder X-ray diffraction patterns of emeraldine base form of PANI and chiral acids doped PANI samples were recorded. Fig. 9 shows the XRD pattern of emeraldine base form of PANI, PANI-(+)-HCSA and PANI-Dibenzoyl-D-Tr. PANI-(+)-HCSA and PANI-Dibenzoyl-D-Tr which have orthorhombic symmetry with space group *pbcn* [36, 37]. The broad diffused peak at approximately 19° indicates that the morphology of PANI is amorphous while the powder X-ray patterns of PANI-(+)-HCSA and PANI-Dibenzoyl-D-Tr show a remarkable crystallinity. The Le-Bail fit [38] of the powder X-ray diffraction pattern of the PANI-(+)-Tr ($a = 14.9107 \text{ \AA}$, $b = 6.7752 \text{ \AA}$, $c = 19.7158 \text{ \AA}$, $\alpha = 90.16^\circ$, $\beta = 125.57^\circ$, $\gamma = 94.44^\circ$) and PANI-(+)-Mnd ($a = 14.2062 \text{ \AA}$, $b = 6.2980 \text{ \AA}$, $c = 19.6985 \text{ \AA}$, $\alpha = 89.92^\circ$, $\beta = 124.99^\circ$, $\gamma = 95.01^\circ$) is shown in Fig. 10 and Fig. 11, respectively which confirmed the triclinic symmetry with space group *P-1*.

Crystallinity index of the polymeric samples were calculated by employing a formula given by Manjunath et al [39]. The resolution of the peak R, for X-ray diffraction spectrum with heights h_1 and h_2 and minima m_1 is given as below

$$R = (2m_1) / (h_1 + h_2) \quad (1)$$

In case of polymers, where there are more than two peaks as seen in chiral acid doped PANI, all the peaks and minima between them are measured by using the following equation.

$$R = (m_1 + 2m_2 \dots \dots \dots + m_{n-1}) / (h_1 + h_2 \dots \dots \dots + h_n) \quad (2)$$

where m_1 , m_2 are the heights of minima between two peaks and h_1 , h_2 are the heights of peaks from the base line. The crystalline peaks of PANIs (undoped and doped) are visible in the figures. Hence, for calculating the percentage of crystallinity, appreciably sharp peaks of emeraldine base form of PANI sample at different theta values are considered. Eq. (2) can be reduced for three peaks for such cases as given in equation (3).

$$R = (m_1 + 2m_2) / (h_1 + h_2 + h_3) \quad (3)$$

Then, (1-R) gives the lateral order or the index of crystallinity. The percentage of crystallinity in emeraldine base form of PANI has been estimated by using equation (3). It has been found that pure emeraldine base of PANI is 16% while the crystallinity of chiral acid doped PANI is relatively high. The crystallinity % data of chiral acid doped PANI is presented in Table 2 which indicates that the crystallinity of chiral PANI powder sample may correspond to 100%. Thus, we can easily prepare crystalline PANI by chiral acid doping only.

The broadness of the Bragg reflections clearly indicates the low crystallite size of the product. The crystallite size of the highly crystalline sample was calculated by using Scherer's equation [40] as given below.

$$L_{(hkl)} = (k\lambda) / (\beta \cos \theta) \quad (5)$$

where k is a constant and its value was considered as 0.9 for our calculations, λ is the wavelength of the radiation used (1.54056 \AA), β is the half maximum breadth in radians, and θ is the Bragg's angle.

Table 2. Crystallinity percentage of chiral acid doped PANI

S. No.	Chiral Dopant	Crystallinity (R) %
1	D(-) / L(+)-Tartaric acid	96
2	R(-) / S(+)-Mandelic acid	43
3	R(-) / S(+)-Camphorsulphonic acid	34
4	Dibenzoyl-D-tartaric acid anhydrous	25

The X-ray diffractograms show that PANI doped with D(-) / L(+)-Tartaric acid and R(-) / S(+)-Mandelic acid are highly crystalline while others are highly amorphous. So, the crystal size calculated for D(-) / L(+)-Tartaric acid is 54 nm and for R(-) / S(+)-Mandelic acid is 60 nm while the initially synthesized PANI nanofiber was found to be of 134 nm length. This result indicates that there is almost one third of reduction in fiber length after doping with chiral acids. This result is found in good agreement with our UV-Visible and CD spectral data, which shows that there is an induction of optical activity/helicity in the PANI after doping with chiral acids. Due to this helicity, the structure changes from extended to compact one and finally the length of fiber decreases. But it is not true, infact after doping structure becomes compact and hence the overall length of fiber remains same but the crystallite size decreases. It seems that the straight chain of polymer is converted into a coiled or spring like structure. The % of crystallinity of PANI doped with different chiral acids have been calculated which indicates that as the steric hindrance due to moieties (R) attached on main chain increases, the induction in helicity and crystallinity increases. It happens only

because; the more bulky group on chiral acid has more tendencies to induce helicity/optical activity. The polymer structure changes from extended to compact coil.

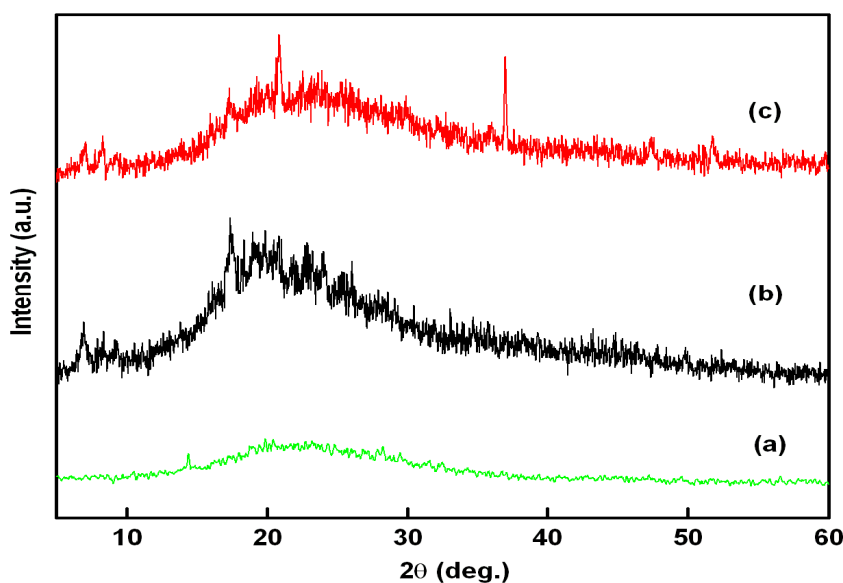


Fig. 9. Powder X-ray diffraction pattern of (a) PANI-EB (b) (+)-HCSA doped PANI(c) O'O-Dibenzoyl-D-Tr acid doped PANI

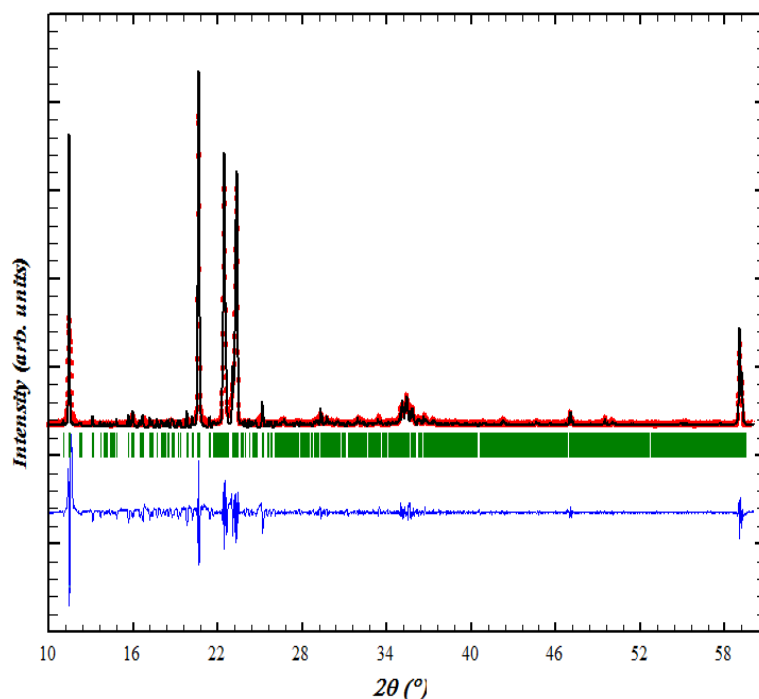


Fig. 10. Le-Bail fit of the powder X-ray diffraction pattern of (+)- Tr acid doped PANI

The compact structure is more closely packed and hence they are more crystalline. On the other hand, the crystal symmetry for emeraldine base form of PANI is orthorhombic and the space group is *pbcn* which is found in agreement with literature value [41]. But after doping with chiral acids, the crystal symmetry changes from orthorhombic to triclinic system and the space group from *pbcn* to *P-1*. The change in crystal symmetry reveals that initially synthesized fiber is symmetrical while after doping with chiral acids, it becomes less symmetrical or asymmetrical. It shows that the asymmetry is due to the induction of helicity in the fibers of PANI. PANI has C_1 schonflies point group while doped PANI has D_{2h} . Chiral crystal point groups 222 is present in chiral acid doped PANI, which shows that it is optically active while no such group is found in PANI. So, the initial plane of attack of PANI and dextro dopants are believed to be similar hence there is faster induction and more attack with better helicity. It reveals that an intrinsic crystal structure of dextro dopant is more favorable for attacking at PANI. Hence,

the relative concentration of dextro dopant is more for attacking at PANI than laevo dopant. These results are found in agreement with the UV-Visible and CD spectral data, which further indicates that there is an induction of optical activity/helicity after doping with the chiral acids. Thus, it can be inferred that the helical PANI is asymmetrical and found more crystalline than undoped PANI.

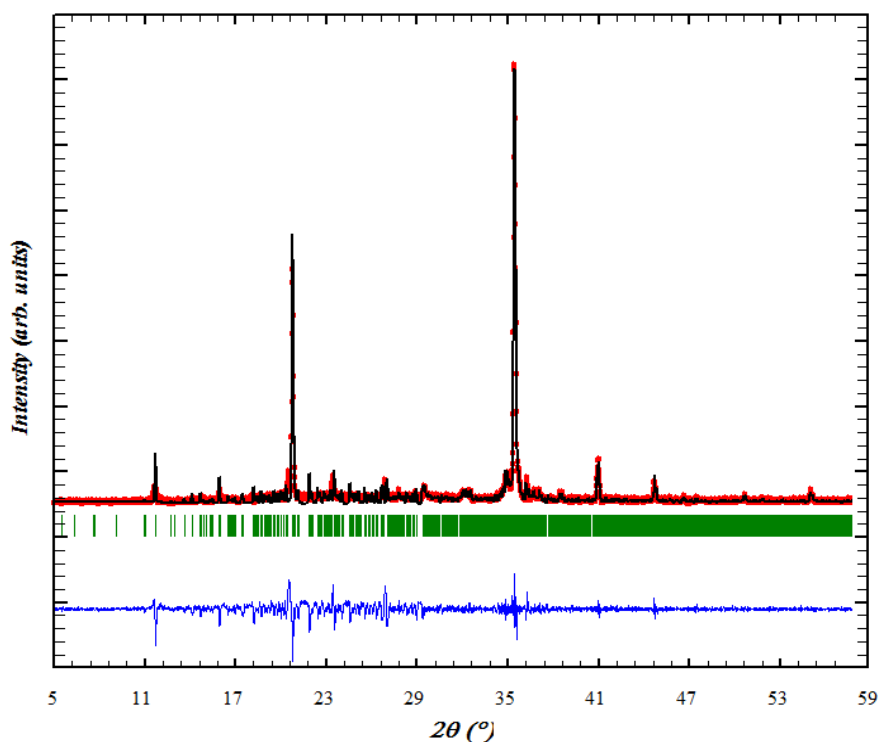


Fig. 11. Le-Bail fit of the powder X-ray diffraction pattern of (+)-Mnd acid doped PANI

Scanning Electron Micrograph

In order to establish the nanofibrillar and helical nature of PANI-EB and PANI doped with Dibenzoyl-D-Tr acid, the morphological behavior has been studied by using SEM technique as a key tool. The SEM micrographs of PANI and PANI-Dibenzoyl-D-Tr are reported in the present work as shown in Fig. 12. SEM micrographs show that the PANI is fibrous while there is a strong coiling between the two fibers of PANI after doping with chiral dopants. It is believed that the secondary forces are playing a key role here for the induction of helicity. A twisting between the two fibers is ruled out because it should have present in the bundle's form or long chain mingling.

On the basis of these facts, it is postulated that the optical activity in chiral acid doped PANI materials arises from individual PANI chain preferentially adopting a one-handed helical screw depending on the hydrogen bonding between the PANI chains and the enantiomeric dopant anions.

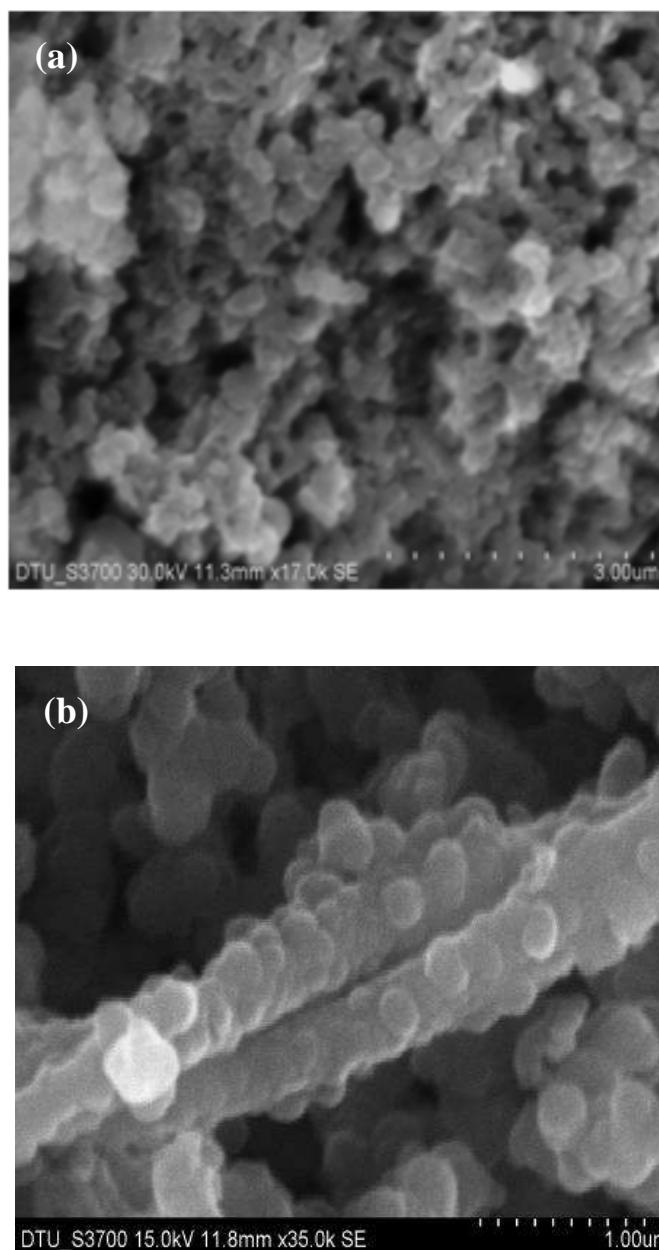


Fig. 12. SEM micrographs of (a) PANI and (b) PANI-Dibenzoyl-D-Tr salt

CONCLUSION

On the basis of the band gap calculated from the spectroscopic data, it is concluded that the optically active PANI salts have higher conductivity than the PANI emeraldine base. It is also seen that the induction of helicity is faster in dextro chiral agents than their corresponding laevo enantiomer because of less energy requirement for structural/conformational changes. The visually observed faster induction of helicity in dextro sample is also confirmed by their band gap data. It is also seen that the optically active PANI salts are more crystalline than PANI emeraldine base and the symmetry changes from orthorhombic to triclinic with space group *pcn* to *P-1*. A chiral crystal point group 222 is present in chiral acid doped PANI. The SEM micrograph of PANI-Dibenzoyl-D-Tr shows that there is a strong coiling between the two fibers of PANI after doping with chiral dopant.

From all these results it is inferred that the initial plane of attack of PANI and dextro dopants are believed to be similar. The hydrogen bonding and electrostatic interaction between two polar sites of chiral dopants and polymer is playing an important role for induction and twisting in the polymer chains. Further, chemical structure of dopant and spatial arrangement of atoms within a dopant is the major molecular property for control of induction in the polymer backbone which is clear established by the use of dextro and laevo dopants in the present study.

Acknowledgements

Authors are thankful to Prof. P B Sharma, Vice-Chancellor, Delhi Technological University (formerly Delhi College of Engineering), Delhi for encouragement and support. A financial support to one of the author, Sudha is also acknowledged gratefully.

REFERENCES

- [1] J. H. Burroughes, D. D. C. Bradley, A. R. Brown, R. N. Marks, K. Mackay, R. H. Friend, P. L. Burns, A. B. Holmes, *Nature*, **1990**, 347, 539.
- [2] M. Trojanowicz, *Microchim. Acta.*, **2003**, 143, 75.
- [3] S. S. Mansoor, A. M. Hussain, K. Aswin, K. Logaiya and P. N. Sudhan, *Der Chemica Sinica*, **2012**, 3, 683.
- [4] A. D. Patel, N. K. Prajapati, S. P. Patel, G. R. Patel, *Der Chemica Sinica*, **2011**, 2(2), 130.
- [5] Y. S. Patel, H. S. Patel, *Der Chemica Sinica*, **2011**, 2(6) 58.
- [6] S. M. Shah, F. B. Bux, V. Parmar, A. Singh, *Der Chemica Sinica*, **2011**, 2(6), 304.
- [7] T. Nakashima, D. Kumar, W. Takashima, T. Zama, S. Hara, S. Sewa, K. Kaneto, *Curr. Appl. Phys.*, **2005**, 5, 202.
- [8] D. Kumar, R. C. Sharma, *Eur. Polym. J.*, **1998**, 34, 1053.
- [9] E. S. Gil, S. M Hudson, *Prog. Polym. Sci.*, **2004**, 29, 1173.
- [10] A. Dholakia, K. Patel H. Trivedi, *Der Chemica Sinica*, **2011**, 2 (3), 106.
- [11] E. Yashima, K. Maeda, Y. Furusho, *Acc. Chem. Res.*, **2008**, 41, 1166.
- [12] Sudha, D. Kumar, M. Iwamoto, *J Appl. Polym. Sci.*, **2013**, 127, 3693.
- [13] Sudha, D. Kumar, M. Iwamoto, *Polym. J*, DOI: PJ.2012.127
- [14] D. B. Amabilino, E. Ramos, J-L. Serrano, T. Sierra, J. Veciana, *J. Am. Chem. Soc.*, **1998**, 20, 9126.
- [15] L. A. P. Kane-Maguire, G. G. Wallace, *Chem. Soc. Rev.*, **2010**, 39, 2545.
- [16] T. Nakano, Y. Okamoto, *Chem. Rev.*, **2001**, 101, 4013.
- [17] R. J. M. Nolte, *Chem. Soc. Rev.*, **1994**, 23, 11.
- [18] A. Kikuchi, T. Okano, *Prog. Polym. Sci.*, **2002**, 27, 1165.
- [19] E. Peeters, M. P. T. Christiaans, R. A. J. Janssen, H. F. M. Schoo, H. P. J. M. Dekkers, E. W. Meijer, *J. Am. Chem. Soc.*, **1997**, 119, 9909.
- [20] L. Pu, *Macromol. Rapid Commun.*, **2000**, 21, 795.
- [21] A. G. MacDiarmid, R. B. Kaner, Handbook of conducting polymers. In: Skotheim TA, editor. New York: Skotheim Marcel Dekker, Inc., **1986(1)**, p.718.
- [22] G. Gustafsson, Y. Cao, G. M. Treacy, N. Colaneri, A. J. Heeger, *Nature*, **1992**, 357, 477.
- [23] K. Maeda, E. Yashima, *Top. Curr. Chem.*, **2006**, 265, 47.
- [24] R. L. Elsenbaumer, H. Eckhardt, Z. Iqbal, J. Toth, R. H. Baughman, *Mol. Cryst. Liq. Cryst.*, **1985**, 118, 111.
- [25] S. A. Ashraf, L. A. P. Kane-Maguire, M. R. Majidi, S. G. Pyne, G. G. Wallace, *Polymer*, **1997**, 38, 2627.
- [26] Y. Pornputtkul, L. A. P. Kane-Maguire, G. G. Wallace, *Macromolecules*, **2006**, 39, 5604.
- [27] L. A. P. Kane-Maguire, G. G. Wallace, *Chem. Soc. Rev.*, **2010**, 39(7), 2545.
- [28] I. D. Norris, L. A. P. Kane-Maguire, G. G. Wallace, *Macromolecules*, **2000**, 33, 3237.
- [29] S-J. Su, M. Takeishi, N. Kuramoto, *Macromolecules*, **2002**, 35, 5752.
- [30] M. Bodner, M. P. Espe, *Synth. Met.*, **2003**, 136, 403.
- [31] C. Boonchu, L. A. P. Kane-Maguire, G.G. Wallace, *Synth. Met.*, **2003**, 136, 241.
- [32] S. Sharma, D. Kumar, *Indian J. Eng. Mater. Sci.*, **2010**, 17, 231.
- [33] J. Libert, J. L. Bredas, A. J. Epstein, *Physical Review B*, **1995**, 51(9), 5711.
- [34] S. F. S. Draman, R. Daik, M. Ahmad, *Malay. Polym. J.*, **2009**, 4(1), 7.
- [35] L. A. P. Kane-Maguire, A. G. MacDiarmid, I. D. Norris, G. G. Wallace, W. Zheng, *Synth. Met.*, **1999**, 106, 171.
- [36] S. Saravanana, C. Joseph Mathaia, M. R. Anantharamana, S. Venkatachalamb P.V. Prabhakaran, *J. Phy. Chem. Solids*, **2006**, 67, 1496.
- [37] H. K. Chaudhari, D. S. Kelkar, *J. App. Polym. Sci.*, **1996**, 15.
- [38] A. L. Bail, H. Duroy, J. L. Fourquet, *Mater. Res. Bull.*, **1988**, 23, 447.
- [39] B. R. Manjunath, A. Venkataraman, *J. Appl. Polym. Sci.*, **1973**, 17, 1091.
- [40] L. E. Alexander, X-ray Diff. Methods in Polymer Science, Wiley- Interscience, John Wiley & Sons, Inc., **1969**, 423.
- [41] J. P. Pouget, M. E. Jdzefowicz, A. J. Epstein, X. Tang, A. G. MacDiarmid, *Macromolecules*, **1991**, 24(3), 779.